JOURNAL OF AIRCRAFT
Vol. 54, No. 6, November–December 2017

Design Forum

DESIGN FORUM papers range from design case studies to presentations of new methodologies to speculations about emerging design trends. They vary from 2500 to 12,000 words (where a figure or table counts as 200 words). Following informal review by the Editors, they may be published within a few months of the date of receipt. Style requirements are the same as for regular contributions (see inside back cover).

Direct Methodology for Constrained System Analysis with Applications to Aircraft Dynamics

Anuj S. Vora* and Nandan K. Sinha†
Indian Institute of Technology Madras, Chennai 600 036, India

DOI: 10.2514/1.C034264

Tools based on the bifurcation and continuation method have been found to be extremely useful for studying multiparameter nonlinear dynamical systems under state and parameter-constrained conditions. Because of inherent limitations of the existing methodologies, however, application of continuation techniques to certain types of problems has remained cumbersome and even computationally challenging. This paper provides an alternate direct approach in MATLAB® using its continuation subroutine MATCONT to extend the capabilities of continuation techniques in an attempt to accommodate a wide variety of constrained dynamics problems. Published results in the literature are first reproduced for validation of the proposed approach. A control problem of scheduling gains for the longitudinal flight dynamics of an aircraft is next presented to show usefulness of the proposed methodology, followed by solutions to an aircraft conceptual design problem involving wing morphing with eigenvalue constraints, with the difficulties of the selected problems increasing in that order.

Nomenclature

b	=	wing span, m
C_D, C_L, C_Y	=	coefficients of drag, lift, and side force, respectively
C_l, C_m, C_n	=	aerodynamic rolling, pitching, and yawing moment coefficients, respectively
c	=	mean aerodynamic chord, m
I_x, I_y, I_z	=	roll, pitch, and yaw moments of inertia, kg · m^2
Ma	=	Mach number
m	=	mass of aircraft, kg
p, q, r	=	body axis roll, pitch, and yaw rates, respectively, deg/s
S	=	wing planform area, m^2
T_m	=	maximum available engine thrust, N
V	=	velocity of aircraft, m/s
α, β	=	angle of attack and sideslip angle, respectively, deg
$\delta e, \delta a, \delta r$	=	elevator, aileron, and rudder deflection angles, respectively, deg
η	=	thrust as fraction of maximum available thrust
μ, γ	=	wind-axis angles, deg
ρ	=	air density, kg/m^3
ϕ, θ	=	Euler bank and pitch angles, respectively, deg

I. Introduction

DYNAMICS of many physical systems from science and engineering are governed by a set of nonlinear ordinary differential equations,

$$\dot{\boldsymbol{x}} = \boldsymbol{f}(\boldsymbol{x}, \boldsymbol{U}) \tag{1}$$

where $\boldsymbol{x} \in \Re^n$ is the vector of n-state variables of the system, $\boldsymbol{U} \in \Re^m$ is the vector of m-control parameters, $\boldsymbol{f}$ is the nonlinear vector field governing system dynamics, and a dot over $\boldsymbol{x}$ indicates the time derivative of $\boldsymbol{x}$. For a set of fixed parameters, $\boldsymbol{U} = \boldsymbol{U}_0$, the system of equations (1) can be integrated from a chosen initial condition, $\boldsymbol{x}(t = 0) = \boldsymbol{x}(0)$, to study the time evolution of $\boldsymbol{x}$. This procedure can be repeated an infinite number of times, starting from different initial conditions for an innumerous fixed combination of parameters values in order to thoroughly examine system dynamics. This is undoubtedly an exhaustive and cumbersome exercise, a major problem with this exercise being the selection of initial conditions, which is a nontrivial task when dealing with systems that are nonlinear. An alternate and more efficient approach to analyzing nonlinear dynamical systems [Eq. (1)] is based on the asymptotic bifurcation and continuation method. The bifurcation and continuation method begins with the computation of steady states of the equilibrium type of Eq. (1), which amounts to solving the set of simultaneous algebraic equations

$$\dot{\boldsymbol{x}} = \boldsymbol{f}(\boldsymbol{x}, \boldsymbol{U}) = 0 \tag{2}$$

and computing the eigenvalues (governing local dynamics of the system around equilibrium states [1]) of the Jacobian matrix, $J = (\partial \boldsymbol{f}/\partial \boldsymbol{x})$, at each equilibrium state. The numerical scheme to solve both the problems together popularly known as a continuation algorithm is of a predictor–corrector type [2], which is described in the next section in some detail. A continuation algorithm is designed to solve the system of equations (2) as a function of a single parameter of the system $u \in \boldsymbol{U}$, known as the continuation parameter, while it

Received 21 October 2016; revision received 26 February 2017; accepted for publication 4 March 2017; published online Open Access 18 May 2017.

*Masters Student, Department of Aerospace Engineering; anujvora@iitb.ac.in.

†Professor, Department of Aerospace Engineering; nandan@ae.iitm.ac.in.

requires remaining $(m-1)$ parameters $\boldsymbol{p}$ of $\boldsymbol{U}$ to remain fixed at their starting values, the equivalent system of equations to be solved thus being

$$\dot{\boldsymbol{x}} = \boldsymbol{f}(\boldsymbol{x}, u, \boldsymbol{p} = \text{fixed}) = 0 \tag{3}$$

Other types of problems may require $\boldsymbol{p}$ varying as some (predefined or arbitrary) functions of the continuation parameter as $\boldsymbol{p} = \boldsymbol{p}(u)$, the equivalent system of equations being solved in this case being

$$\dot{\boldsymbol{x}} = \boldsymbol{f}[\boldsymbol{x}, u, \boldsymbol{p} = \boldsymbol{p}(u)] = 0 \tag{4}$$

Solutions of Eqs. (3) and (4) are classified as parameter-constrained equilibrium states of the system. The other type of equilibrium states is state-constrained equilibrium states, which, as the name itself suggests, are required to satisfy certain constraints on the states of the system. The system of equations to be solved in this case is

$$\boldsymbol{f}(\boldsymbol{x}, \boldsymbol{U}) = 0; \qquad \boldsymbol{g}(\boldsymbol{x}) = 0 \tag{5}$$

The k constraint equations, $g_i(\boldsymbol{x}) = 0$, $i = 1, \ldots, k$, added to the original set of n algebraic Eq. (2) (representing equilibrium states of the system), require $(n + k)$ algebraic equations to be solved together now for the equilibrium states that satisfy the imposed constraint relations. Direct equality constraints such as the type in Eq. (5) and indirect equality constraints, for example, based on control of time response characteristics via feedback-control parameters or system design parameters (both attempted later as illustrative example problems), can be attempted within the framework of continuation methodologies. An extended bifurcation analysis (EBA) procedure proposed by Ananthkrishnan and Sinha [3] was found to be useful for trim and stability analysis of systems under state-constrained conditions. The two-step EBA procedure involved computing parameter schedules, $p_i(u)$, $i = 1, 2, \ldots k$, first, which kept the system in equilibrium states satisfying the constraints $g_i(\boldsymbol{x}) = 0$, $i = 1, \ldots, k$, and afterward carrying out another continuation of the system model augmented with the parameter schedules [as in Eq. (4)] in the second step. Details of the EBA procedure can be found in [4]. Carrying out EBA continuation particularly in the popularly used AUTO [5] continuation framework requires overcoming several roadblocks in handling systems with constraints. Foremost among them is 1) the requirement of an extremely accurate starting point (steady state) to begin the continuation in general for any problem (otherwise, continuation may not start or terminate abruptly) and 2) that for constrained system analysis the second step of the EBA requires another continuation, which runs into two further problems. The first is, again, the need for an accurate starting point that satisfies the constraints on the state(s), and the second is the inclusion of parameter schedules computed in the first step, either in the form of a polynomial fit with a certain degree of smoothness or a lookup table, needing an interpolation. The need for a methodology that overcomes the previously mentioned problems has therefore always existed.

In this paper, a direct continuation methodology that overcomes all of the issues listed previously, with a minor modification in the continuation procedure, is proposed. The direct methodology eliminates the need for the second step of the EBA procedure and enables one to deal with problems that could not be studied under the framework of the EBA procedure, thereby extending the scope of the continuation-algorithm-based methodologies. The direct methodology is implemented in the MATLAB®-based continuation subroutine MATCONT [6], which allows users further access to a host of other subroutines in MATLAB, thus making it possible to apply both direct constraints, represented by explicit constraint equations, and indirect constraints on the system.

Three different example problems illustrating usefulness of the direct methodology have been attempted in this paper. The methodology is first applied to study constrained dynamics of the F-18 high angle-of-attack research vehicle (HARV) model in a level-flight trim condition, and the results are validated against those available in the literature. The second example shows the implementation of the direct methodology to automate gain scheduling of a simple feedback-control law for the longitudinal dynamics of the F-18/HARV model over the entire range of level-flight trims. Computing wing configuration parameters for an airplane in flight, required for satisfying handling qualities requirements over the entire range of level-flight trims, is taken up as the third example problem.

The paper is organized as follows. Section II presents basic descriptions of a continuation algorithm and the proposed direct continuation methodology. Illustrative examples of the application of the direct methodology to aircraft flight dynamics problems are presented in Sec. III, and in Sec. IV, concluding remarks with future directions of work are presented.

II. Basic Description of Numerical Continuation Algorithm

A continuation algorithm is essentially based on computing steady states of the system of equations (2) as a function of one of the system parameters,

$$\boldsymbol{f}(\boldsymbol{x}^*, u^*, \boldsymbol{p}) = 0 \tag{6}$$

where $u \in \boldsymbol{U}$ is the varying parameter, also known as the continuation parameter, and $\boldsymbol{p} \in \boldsymbol{U}$ are other parameters kept fixed in a continuation; the asterisk indicates the equilibrium condition. Continuation with respect to the parameter u marches from a given starting solution point [satisfying Eq. (6)] following a predictor–corrector marching scheme, finally resulting in a solution branch $\boldsymbol{x}^* = \boldsymbol{x}^*(u^*)$. Along a continuation path, the Jacobian matrix $(\partial \boldsymbol{f}/\partial \boldsymbol{x})$ needs to be evaluated at each equilibrium point, the eigenvalues of which, simultaneously computed, mark the stability of the equilibrium points all along the solution branch. For this to happen, a necessary condition is that $\boldsymbol{f}$ must be smooth (at least C^1 continuous) as demanded by the implicit-function theorem [7]. Along a continuation path, the singularity of $(\partial \boldsymbol{f}/\partial \boldsymbol{x})$ at an equilibrium point corresponding to the critical value of the continuation parameter $u = u_{\text{cr}}$, known as the bifurcation point, results in a change in stability and/or the number of equilibrium solutions. Additional solution branches emerge from bifurcation points depending on the type of loss of stability [8], which advanced continuation algorithms, such as AUTO, are designed to identify and compute in a continuation. Comprehensive details of numerical aspects of a continuation algorithm can be found in [2]. Several types of bifurcations of different types of steady states (equilibrium, periodic, toroidal, quasi-periodic, and so on) of nonlinear dynamical systems described by Eq. (1) and the resulting onset of new types of solutions [1,8] can all be captured in a continuation run as functions of u, thus revealing the global dynamic behavior of a system with respect to u. Further, a continuation algorithm can also handle Eq. (6) augmented with equality constraints of the type

$$\boldsymbol{g}(\boldsymbol{x}^*, u^*, \boldsymbol{p}) = 0 \tag{7}$$

as long as Eqs. (6) and (7) are coupled and the numerical problem is well defined. This translates into the requirement that there must be at least as many parameters available in $\boldsymbol{p}$ as the number of added constraint equations, and the parameters used in a continuation of Eqs. (6) and (7) must influence the constraints [3]. Currently available continuation algorithms are not designed to distinguish between equations of steady states and equality constraint equations; therefore, they compute the Jacobian matrix of the system of equations (6) and (7) together in a continuation, which is given by

$$J(\boldsymbol{x}, u, \boldsymbol{p}_1, \boldsymbol{p}_2) = \begin{pmatrix} \boldsymbol{f}_{\boldsymbol{x}}(\boldsymbol{x}, u, \boldsymbol{p}_1, \boldsymbol{p}_2) & \boldsymbol{f}_{\boldsymbol{p}_1}(\boldsymbol{x}, u, \boldsymbol{p}_1, \boldsymbol{p}_2) \\ \boldsymbol{g}_{\boldsymbol{x}}(\boldsymbol{x}, u, \boldsymbol{p}_1, \boldsymbol{p}_2) & \boldsymbol{g}_{\boldsymbol{p}_1}(\boldsymbol{x}, u, \boldsymbol{p}_1, \boldsymbol{p}_2) \end{pmatrix} \tag{8}$$

In Eq. (8), $\boldsymbol{p}_1$ is the vector of parameters from $\boldsymbol{U}$ to be used as additional variables to make the continuation problem well defined, while $\boldsymbol{p}_2$ are remaining parameters still to be kept fixed. Once the problem is well defined, continuation with u can be carried out as before; however, the eigenvalues of the inflated Jacobian matrix due to additional equations of constraints do not result in correct stability

information of the constrained equilibrium solutions, which is still based on the eigenvalues of the (1,1) entry of Eq. (8) alone. This problem can be solved by extracting the (1,1) entry from Eq. (8) along a continuation and computing eigenvalues of (1,1) separately. This procedural change, though minor, overcomes the major limitation of using the continuation algorithm in carrying out trim and stability analysis of dynamical systems represented by Eq. (1) in constrained conditions. This direct procedure not only helps get rid of the a priori scheduling of $\boldsymbol{p}_1$ as function of u (requiring interpolation or polynomial fitting), but it also completely gets rid of the second step of the EBA technique, except that solution branches originating at bifurcation points cannot not be computed now; this procedure computes only solutions satisfying the equality constraints. A second continuation run may still be needed if one were interested in computing bifurcated solution branches (the procedure explained in [3]), but if there is no such requirement (and, indeed, that is the case with many practical problems), one may solve a host of problems related to constrained cases using this small change in procedure itself. The advantages of using MATCONT over AUTO continuation algorithm becomes obvious here for the simple reason that various MATLAB subroutines can be directly incorporated in MATCONT and a variety of problems solved as we will see in the example cases presented in this paper. Spetzler and Narang-Siddharth [9] used a similar methodology in COSY, a proprietary continuation code, to perform constrained analysis of multiparameter dynamical systems. Their paper also suggested a method to trace out the solution branches emanating from a bifurcation point. The procedure is explained here for the sake of completeness.

The presence of bifurcation points on an equilibrium curve suggests the existence of additional solution branches emerging from the bifurcation points. These solution branches also follow the same parameter schedules; however, these branches do not obey the constraints imposed on the system and are therefore termed off-nominal solutions. Off-nominal solution branches can be computed in a second continuation by solving the augmented set of equations

$$\boldsymbol{F}(\boldsymbol{x}, \boldsymbol{y}, u, \boldsymbol{p}) = \begin{pmatrix} \boldsymbol{f}(\boldsymbol{y}, u, \boldsymbol{p}) \\ \boldsymbol{f}(\boldsymbol{x}, u, \boldsymbol{p}) \\ \boldsymbol{g}(\boldsymbol{x}, u, \boldsymbol{p}) \end{pmatrix} = 0 \tag{9}$$

where the state variables $\boldsymbol{x}$ trace the nominal solution branches satisfying the constraints $\boldsymbol{g}(\boldsymbol{x}, u, \boldsymbol{p}) = 0$, while the dummy state variables $\boldsymbol{y}$ trace the off-nominal solution branches.

The described methodology was implemented in MATCONT, which is an open-source continuation toolbox in the MATLAB computing environment. The source code was appropriately modified to enable constrained bifurcation analysis as well as the tracing of branching solutions. In the following sections, three different constrained aircraft flight dynamics problems are attempted to illustrate the usefulness of the methodology. Among selected problems, the first one is for validation of the methodology against the results available in literature, and the other two are new applications.

III. Applications of Direct Continuation Methodology to Aircraft Flight Dynamics

A. State-Constrained Maneuver Analysis

Aircraft most often fly maneuvers that are constrained in states. Multiple available controls are deployed simultaneously to keep an aircraft in constrained trim states. One of the most basic maneuvers of aircraft is the cruise (level) flight condition. In a cruise flight condition, aircraft are required to fly straight (sideslip angle, $\beta = 0$ deg), at constant altitude (flight-path angle, $\gamma = 0$ deg), and with wings level (bank angle, $\phi = 0$ deg).

To compute all possible trims and the stability of trims for an aircraft within prescribed limits of control inputs, i.e., to investigate global dynamics of aircraft in the cruise flight condition, the direct methodology is applied to the equations,

$$\dot{\boldsymbol{x}} = \boldsymbol{f}(\boldsymbol{x}, \delta e, \delta a, \delta r, \eta) = 0; \quad \beta = 0; \quad \gamma = 0; \quad \phi = 0 \tag{10}$$

In Eq. (10), the first set of algebraic equations represents aircraft six degrees-of-freedom rigid-body motion equations (given in the Appendix) set to zero for the steady state, and other equality relations are constraint equations. The aircraft chosen for this analysis is F-18/HARV available in the public domain. Inertia and geometric properties of the F-18/HARV model along with aerodynamic data available in the angle-of-attack range $-4 \leq \alpha \leq 90$ deg complete the model [10]. A continuation of Eq. (10), with elevator deflection angle δe varying as the continuation parameter and throttle η, aileron deflection angle δa, and rudder deflection angle δr also varying along simultaneously, to keep the states constrained as required [3], is now directly carried out. Further, in this case, off-nominal solution branches are also computed using the procedure outlined in Sec. II. Results of the continuation are plotted in Figs. 1a–1c.

State variables plotted in Fig. 1a are all constrained as seen from sideslip angle β and bank angle ϕ plots and the flight-path angle γ plot in Fig. 1b; nominal values of all three variables are zero as demanded by the constraints. Loss of aircraft stability in the level-flight condition is marked by the presence of Hopf bifurcation and pitchfork bifurcation points at critical elevator deflection angles as indicated on the α–δe plot in Fig. 1a.

The throttle η required schedule against elevator deflection δe with stability information resulting from direct computation is also plotted in Fig. 1b. Minimum thrust required (corresponding to minimum drag) level-flight trim with stability, a useful performance indicator, can be directly read from the plot. These results for F-18/HARV, obtained using the direct continuation, match the results available in [10] obtained by using the EBA procedure. A loss in stability and resulting bifurcations at critical angles of attack are due to the phugoid and spiral mode eigenvalues as seen from the root locus plot in Fig. 1c. Root locus plots useful in control design (next example) and performance plots useful for aircraft designers are simultaneous outcomes of the direct continuation, which succinctly shows usefulness of the direct methodology. Off-nominal solution branches show departure from the level trim state, in this case spiral divergence, as one would expect from a single real (spiral mode) eigenvalue crossing zero resulting in a static bifurcation [1].

B. Gain Scheduling

Stability losses for F-18/HARV in the level-flight condition in the previous example were identified to be due to phugoid and spiral modes, as shown in Fig. 1c (marked by the real part of eigenvalues crossing zero from below). These modes can be stabilized locally at a trim state with the help of a feedback-control law, the process known as stability augmentation [11]. For aircraft, stability augmentation is also needed for handling and flying quality requirements, which demand that aircraft transient behavior in the whole range of trims in a particular flight condition be identical or within some bounds [12]. There are various methods for stability-augmentation-control design, and based on the technique used, they can be classified as linear or nonlinear. In linear control, the input is proportional to the linearized output, and it is widely used due to the ease of implementation. However, recently researchers have also used nonlinear flight-control design techniques such as robust control [13] and sliding mode control [14] in the entire flight envelope to ensure appropriate handling qualities in the presence of model uncertainties. In this paper, the design of linear feedback-control laws for two tasks, first for assigning the short-period mode eigenvalues as desired by handling and flying qualities and second for keeping the short-period mode eigenvalues at the desired location for all level-flight trims, is carried out as a second example problem to show the usefulness of the direct continuation methodology. Some basics of feedback-control law design methodology are presented next.

Consider a linearized system written in the state-space form as

$$\Delta\dot{\boldsymbol{x}} = A\Delta\boldsymbol{x} + B\Delta\boldsymbol{u} \tag{11}$$

$$\boldsymbol{y} = C\Delta\boldsymbol{x} \tag{12}$$

where $\boldsymbol{x} \in \Re^n$ is the state vector, $\boldsymbol{u} \in \Re^m$ is the control vector, and $\boldsymbol{y} \in \Re^r$ is the output vector. $A \in \Re^{n\times n}$ is the Jacobian matrix of the

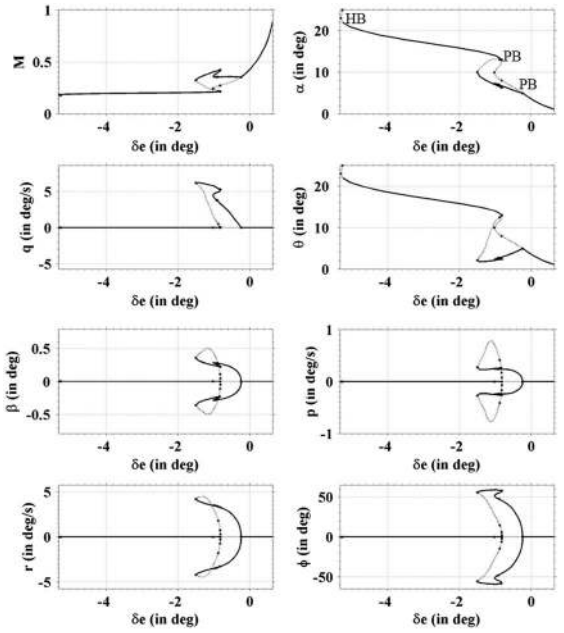

a) Bifurcation plots for F-18/HARV in straight and level-flight condition (solid lines: stable trims, dotted lines: unstable trims, HB: Hopf bifurcation, PB: pitchfork bifurcation)

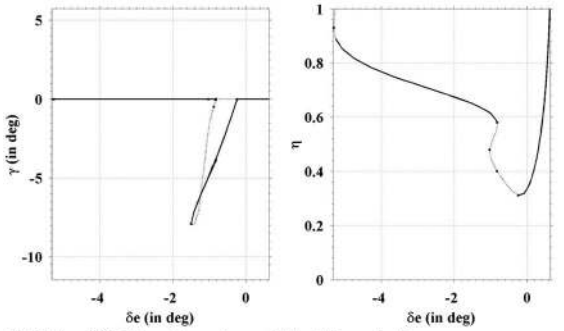

b) Plots of flight-path angle and throttle variation with elevator deflection angle

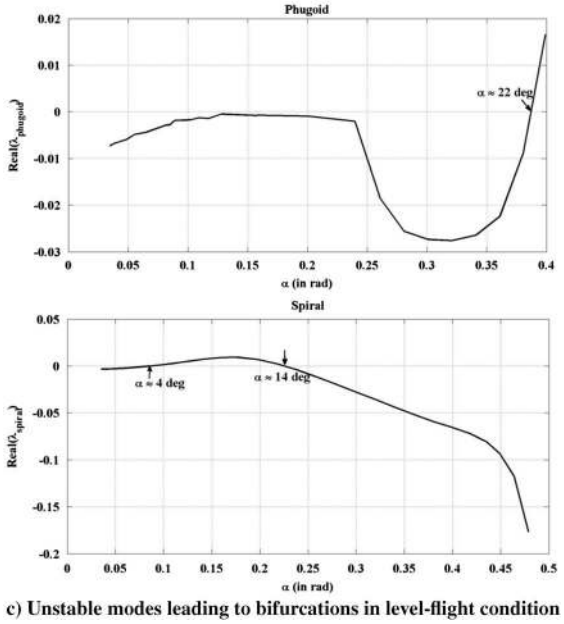

c) Unstable modes leading to bifurcations in level-flight condition

Fig. 1 Bifurcation diagrams and root locus plots of F-18/HARV in straight and level flight trim condition.

system evaluated at a trim condition, also known as the system matrix. $B \in \Re^{n\times m}$ is the control matrix, and $C \in \Re^{r\times n}$ is the output matrix. Δ represents perturbation from the equilibrium condition, for example, $\Delta \boldsymbol{x} = \boldsymbol{x} - \boldsymbol{x}^*$, where $\boldsymbol{x}^*$ is the magnitude of state variables at the equilibrium condition. Consider a full-state feedback law augmented to the system, Eq. (11), as

$$\Delta \boldsymbol{u} = -K\Delta \boldsymbol{x} \tag{13}$$

where $\Delta \boldsymbol{u}$ is the control signal given by $\Delta \boldsymbol{u} = \boldsymbol{u} - \boldsymbol{u}^*$; $\boldsymbol{u}^*$ is the magnitude of the control variable at the equilibrium condition $\boldsymbol{x}^*$. The $K \in \Re^{m\times n}$ matrix is known as the feedback gain matrix, which determines the control response to the perturbation. A simple control input for the case in which $n = 2$ and $m = 1$ results in

$$\Delta u = -(k_1 \Delta x_1 + k_2 \Delta x_2) \tag{14}$$

The corresponding closed-loop system can then be represented as

$$\Delta \dot{\boldsymbol{x}} = (A - BK)\Delta \boldsymbol{x} \tag{15}$$

A fundamental theorem in modern control theory states that if a system is controllable, i.e., the rank of the matrix $\kappa = [\,B \quad AB \quad A^2B \quad \cdots \quad A^{n-1}B\,]$ is n, where n is the dimension of the system, then there exists a gain matrix such that the eigenvalues of the closed-loop system, Eq. (15), can be assigned exactly as desired. However, in general, it is neither feasible nor required to feedback all the states. Usually, only the measured variables are used as feedback elements, resulting in the output feedback-control law:

$$\Delta \boldsymbol{u} = -Ky = -KC\Delta \boldsymbol{x} \tag{16}$$

The corresponding closed-loop system is

$$\Delta \dot{\boldsymbol{x}} = (A - BKC)\Delta \boldsymbol{x} \tag{17}$$

It is an established result that the number of eigenvalues that can be exactly assigned to the system is equal to the rank of the matrix C [15], which also signifies the number of output variables. Generally, in flight-control systems, the variables $\{\alpha, q\}$ are used as measured output for the longitudinal dynamics, and $\{\beta, \bar{p}, r\}$ are used as measured output variables for the lateral dynamics, suggesting ranks 2 and 3, respectively. Thus, two longitudinal dynamics eigenvalues and three lateral-directional dynamics eigenvalues can be controlled by the feedback law in Eq. (16).

As the system is linearized at a particular trim condition, the gains computed will result in the desired response only at that operating trim condition. A change in the trim condition will require a change in the gain values for the same desired controlled response. Thus, it is essential to compute the gains over the whole range of trims in a particular flight condition to ensure that the system has uniform desirable controlled response over the complete range of trims. In control terminology, this exercise is called gain scheduling. A vast amount of literature is available on this topic, discussing various numerical methods of gain scheduling. In this work, a gain-scheduling exercise is carried out using the direct continuation approach for the F-18/HARV model in the level-flight trim condition.

The feedback law is designed with the output variables, $\boldsymbol{y} = [\alpha, q]^T$. The elevator is used as the control parameter, which means that the rank of the matrix is $\text{rank}(B) = 1$. One control parameter associated with two output variables results in two nonzero entries in the gain matrix $K = [0, k_1, k_2, 0]^T$, for longitudinal dynamics of aircraft, where k_1 and k_2 determine the control inputs corresponding to the changes in α and q. Thus, two eigenvalues can be assigned at their desired values. The eigenvalues can be chosen depending on the desired frequency and damping characteristics of the mode. In this example, the desired short-period mode eigenvalues are fixed at $\lambda_{\text{SP}} = \xi_r \pm i\xi_i = -1.5 \pm i1.33$, which is different from the open-loop short-period mode eigenvalues for the F-18 model in the entire range of level-flight trims plotted in Fig. 2.

Keeping short-period eigenvalues fixed at all trims in the level-flight condition amounts to the two constraint functions

$$\boldsymbol{g}(\boldsymbol{x}, u, \boldsymbol{p}) = \begin{pmatrix} \lambda_{r,\text{SP}}(\boldsymbol{x}, u, \boldsymbol{p}) - \xi_r \\ \lambda_{i,\text{SP}}(\boldsymbol{x}, u, \boldsymbol{p}) - \xi_i \end{pmatrix} \tag{18}$$

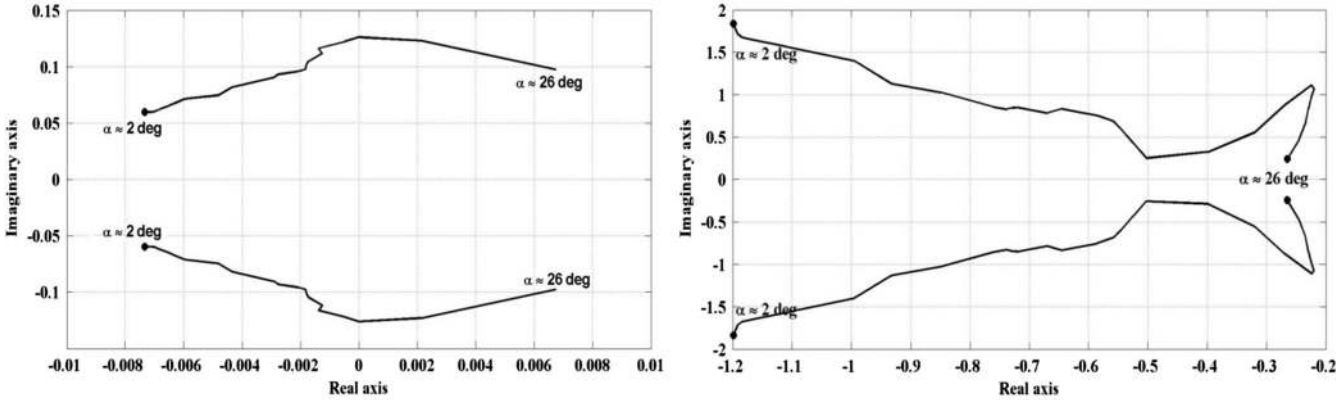

a) Phugoid b) Short period

Fig. 2 Open-loop root locus plots of short-period and phugoid mode eigenvalues for F-18/HARV model in level-flight condition.

which are implicitly (indirect constraints) exercised via the control of eigenvalues of the Jacobian matrix [of entry (1,1) in Eq. (8)] resulting from the simultaneous equation for the level-flight trim states of aircraft as

$$\boldsymbol{F}(\boldsymbol{x}, u, \boldsymbol{p}) = \begin{pmatrix} \boldsymbol{f}(\boldsymbol{x}, u, \boldsymbol{p}) \\ \gamma \\ \lambda_{r,\mathrm{SP}}(\boldsymbol{x}, u, \boldsymbol{p}) - \xi_r \\ \lambda_{i,\mathrm{SP}}(\boldsymbol{x}, u, \boldsymbol{p}) - \xi_i \end{pmatrix} = 0 \tag{19}$$

with $\boldsymbol{x} = (V, \alpha, \beta, \bar{p}, q, r, \phi, \theta)$, $u = \delta_e$, and $\boldsymbol{p} = (\eta, k_1, k_2)$. Since $\boldsymbol{F} \in \Re^{n+3}$, $\boldsymbol{x} \in \Re^n$, $\boldsymbol{p} \in \Re^3$, and $n = 8$, the problem is well defined with the number of equations equal to the number of unknowns. Here, $u \in \Re$ varies as the continuation parameter. To start the continuation, an initial condition is required for all the variables, including the gains. The initial condition, satisfying the equality constraints, Eq. (19) in this case, was determined separately by using the eigenstructure assignment technique presented in [16]. Closed-loop short-period and phugoid mode eigenvalues are plotted in Fig. 3; feedback gain schedules resulting from constrained continuation are plotted in Fig. 4. Figure 3 shows that for all values of level-flight trims short-period mode eigenvalues are fixed at the same desired location. Each point on the and plots in Fig. 4 is the feedback gains corresponding to the level-flight trim conditions in Fig. 1a, ensuring that the short-period mode eigenvalues of the closed-loop system are fixed as desired. The phugoid mode eigenvalues were not controlled in this case. Root locus plot of phugoid mode (as seen from Fig. 3b) is naturally restricted to the left half complex plane, thus, ensuring stability of this mode at all level-flight trims as well. In general, this may not always be the case, and a careful selection of starting gain values may be necessary to keep the closed-loop phugoid mode stable. It is worth pointing out here that the desired short-period

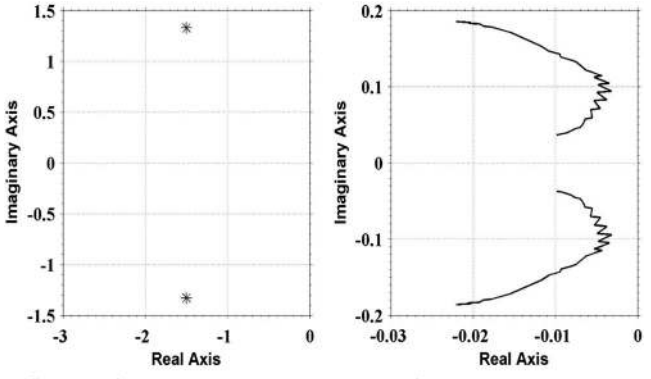

a) Short period b) Phugoid

Fig. 3 Closed-loop short-period and phugoid mode eigenvalues.

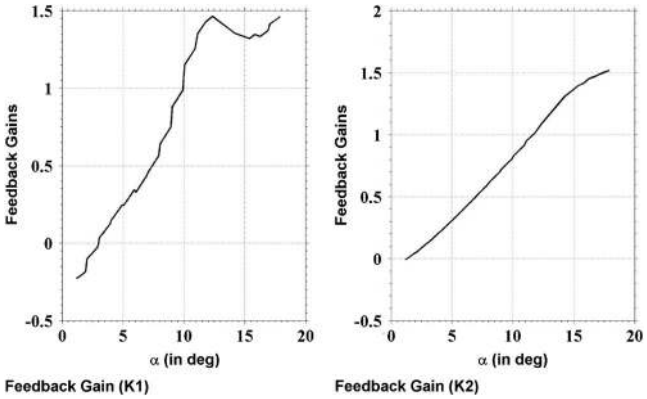

Fig. 4 Closed-loop feedback gains.

eigenvalues are not from the set of open-loop short-period eigenvalues (plotted in Fig. 2), thus showing the generic nature of the selected problem of gain scheduling. Also, the linearization of the aircraft model is part of a continuation at each trim point; system matrix A and control matrix B are automatically generated at each trim point. Alternatively, the gain-scheduling task is carried out by first locating all the trim states of the system, linearizing the system at each trim state, calculating the eigenvalues of the linearized system, and then computing the feedback gains at every trim point [16]. The automated procedure of gain scheduling using the direct continuation methodology thus reduces time and effort significantly.

C. Wing Morphing for Desired Handling Qualities

The gain-scheduling exercise carried out in the previous example to keep the eigenvalues at the desired locations in the whole range of trim points requires an active control system onboard an aircraft. An alternate solution to this problem would be to schedule aircraft configuration parameters themselves so that constraints on eigenvalues are satisfied at all trims in a particular flight condition. This would essentially require changing aerodynamic characteristics of the airplane with changing trims. In this exercise, parameters related to wing shape and orientation are scheduled to place phugoid and Dutch-roll mode eigenvalues of an airplane model at the desired fixed locations; therefore, this exercise is appropriately called wing morphing [17].

Recently, Khatri et al. [18] used a constrained bifurcation and continuation procedure to size horizontal and vertical stabilizers for an airplane based on handling and flying qualities requirements; the task required a large number of repetitive continuation runs. In this work, we extend the design methodology presented in [18] to configure wing parameters based on the handling qualities requirements. As this exercise would require a bare aerodynamic model in terms of wing design variables, we use the same model of a twin turboprop, lightweight, six-seater, business transport aircraft as

used in [18] to illustrate the application of the direct continuation methodology to the wing-morphing problem. Aerodynamics of the aircraft is modeled with the stability derivatives parameterized with respect to wing design variables, thereby suitable for incorporation in the continuation-based methodology. The aerodynamic model, primarily consisting of empirical relations/analytical expressions collected mainly from textbooks [19,20], is a relatively low-fidelity one but adequate enough to demonstrate the capabilities of the direct continuation methodology for the problem at hand.

The design procedure is as follows. First, the aircraft is trimmed at the level-flight trim condition. Constraints on the eigenvalues are formulated as follows:

$$\boldsymbol{g}(\boldsymbol{x}, u, \boldsymbol{p}) = \begin{pmatrix} \lambda_r(\boldsymbol{x}, u, \boldsymbol{p}) - \xi_r \\ \lambda_i(\boldsymbol{x}, u, \boldsymbol{p}) - \xi_i \end{pmatrix} \tag{20}$$

This exercise has been carried out for phugoid and Dutch-roll modes separately to gain better insight into how wing parameters have to be scheduled in the whole range of level-flight trims, even though there may be fringe influence of the parameters on both the modes together. The wing aspect ratio AR_{wing} and wing incidence angle i_{wing} are used as free variables to hold phugoid mode eigenvalues fixed at the desired location, and wing sweep Λ_{wing} and wing dihedral Γ_{wing} angles are used for holding Dutch-roll mode eigenvalues fixed at the desired locations. It is assumed that these parameters do not have significant effects on weight, CG, and moment of inertia values. In both the cases, constraints are implicitly exercised via directly controlling the eigenvalues of entry (1,1) of the inflated Jacobian matrix [Eq. (8)] as was done in the previous case, an exercise conveniently carried out in MATCONT.

1. Constraint Formulation for Phugoid Mode Eigenvalues

The simultaneous equations to be solved together in a continuation in this case are

$$\boldsymbol{F}(\boldsymbol{x}, u, \boldsymbol{p}) = \begin{pmatrix} \boldsymbol{f}(\boldsymbol{x}, u, \boldsymbol{p}) \\ \gamma \\ \lambda_{r,\text{PH}}(\boldsymbol{x}, u, \boldsymbol{p}) - \xi_r \\ \lambda_{i,\text{PH}}(\boldsymbol{x}, u, \boldsymbol{p}) - \xi_i \end{pmatrix} = 0 \tag{21}$$

where

$$\boldsymbol{x} = (V, \alpha, \beta, \bar{p}, q, r, \phi, \theta), \qquad u = \delta_e, \qquad \boldsymbol{p} = (\eta, i_{\text{wing}}, AR_{\text{wing}})$$

2. Constraint Formulation for Dutch-Roll Mode Eigenvalues

The simultaneous equations to be solved together in a continuation in this case are

$$\boldsymbol{F}(\boldsymbol{x}, u, \boldsymbol{p}) = \begin{pmatrix} \boldsymbol{f}(\boldsymbol{x}, u, \boldsymbol{p}) \\ \gamma \\ \lambda_{r,\text{DR}}(\boldsymbol{x}, u, \boldsymbol{p}) - \xi_r \\ \lambda_{i,\text{DR}}(\boldsymbol{x}, u, \boldsymbol{p}) - \xi_i \end{pmatrix} = 0 \tag{22}$$

where $\boldsymbol{x} = (V, \alpha, \beta, \bar{p}, q, r, \phi, \theta)$, $u = \delta_e$, and $\boldsymbol{p} = (\eta, \Gamma_{\text{wing}}, \Lambda_{\text{wing}})$.

IV. Results and Discussions

Three separate continuation runs each for the phugoid mode control and for the Dutch-roll mode control starting from different initial conditions are performed. Frequencies and damping ratios corresponding to the three cases along with the eigenvalues are given in Table 1. They are characteristic values corresponding to three different level-flight trims at $\alpha = 1$ deg (type I), $\alpha = 3$ deg (type II), and $\alpha = 5$ deg (type III). These trim conditions are used as the starting points for the three continuation runs. In each continuation run, the eigenvalues at the starting trim condition are the reference values to be held constant for all other trim solutions. In the first set of computations, the phugoid mode eigenvalues are held constant, while in the second set, the Dutch-roll mode eigenvalues are held constant.

Table 1 Constrained magnitudes of frequency and damping ratio

	Phugoid (case 1)				Dutch-roll (case 2)			
Type	ω_n, rad/s	ζ	λ_r	λ_i	ω_n, rad/s	ζ	λ_r	λ_i
I	0.118	0.129	−0.015	0.117	2.724	0.151	−0.411	2.693
II	0.165	0.080	−0.013	0.164	2.078	0.154	−0.320	2.053
III	0.200	0.070	−0.014	0.200	1.806	0.165	−0.298	1.781

Continuation plots for phugoid mode control are plotted in Figs. 5a–5c. As noticed from Fig. 5a, for all values of trims starting from each of the three starting points given previously, phugoid mode eigenvalues are fixed at the same desired location. There is no control over short-period mode eigenvalues in this exercise; therefore, they move freely, though inside the stable region in the complex plane. The lateral mode eigenvalues are also not controlled, and hence they move freely as well in the complex plane. The roll and the Dutch-roll mode eigenvalues stay in the stable region, but the spiral mode crosses the imaginary axis to become unstable. The spiral mode (as well as roll mode) eigenvalues for the three cases are indistinguishable as they overlap with each other.

Schedules of the wing aspect ratio and wing incidence angle for the phugoid case, the outcome of the continuation runs, turn out to be as shown in Fig. 5b. Stability information, which is a natural outcome of the continuation, is marked on wing parameter schedules as well as on the aircraft-state variables (only longitudinal variables are plotted; lateral directional variables are all zero). Plots of schedules and state variables in Fig. 5b show a stretch of a solid line (consisting of stable level-flight trim solutions) and a connected stretch of a dotted line (representing unstable level-flight trim solutions). Since this whole exercise was carried out using full-order aircraft equations, stability information on these plots corresponds to the location of the eigenvalues of all the modes of aircraft. In all three cases, the unstable trims are due to the spiral mode becoming unstable.

The flight-path angle γ shown in Fig. 5c is zero as demanded by the constraint equation. The Mach number is approximately constant in all three cases for all trims, confirming that fixing the frequency of the phugoid mode for all modes also fixes the trim speed as per the approximate phugoid frequency formula [4], $\omega_n \approx \sqrt{2}(g/V^*)$, which is only dependent on the trim speed. While type I solutions demand higher speeds and equivalently higher throttle settings, solutions for the type I case may not be desirable as the variation in aspect ratio is much larger in comparison to types II and III solutions. Also, in this case, variation in short-period mode parameters is much higher. Hence, an important conclusion derived from this exercise is that types II and III solutions and the corresponding wing aspect ratio/incidence angle schedules may be used for wing morphing for phugoid control. Based on stability considerations, type II schedules have stable trims for a larger range of angle of attack, and hence this is the most suitable solution branch of the three, whereas type III schedules can be recommended for minimum thrust required in the whole range of angles of attack.

The second set of continuation results for control of the Dutch-roll mode eigenvalues is plotted in Figs. 6a–6c. As seen from the root locus plot in Fig. 6a, the Dutch-roll mode eigenvalues are fixed at the desired types I, II, and III values as demanded by the constraints. Roll and spiral modes move freely as no constraints on them have been exercised. For some trim solutions, the spiral mode eigenvalues cross the imaginary axis and become unstable. Spiral mode (and roll mode) eigenvalues for the three cases overlap and are hence indistinguishable. The longitudinal mode eigenvalues, which are unconstrained, move freely in the stable region of the complex plane, showing the significant influence of wing dihedral and sweep angles on the longitudinal dynamic modes. It is important to point out here that the empirical data required to model the dihedral and the sweep angles in the aerodynamics of the aircraft were limited to positive angles. Therefore, the trims corresponding only to the positive dihedral and sweep angles are plotted.

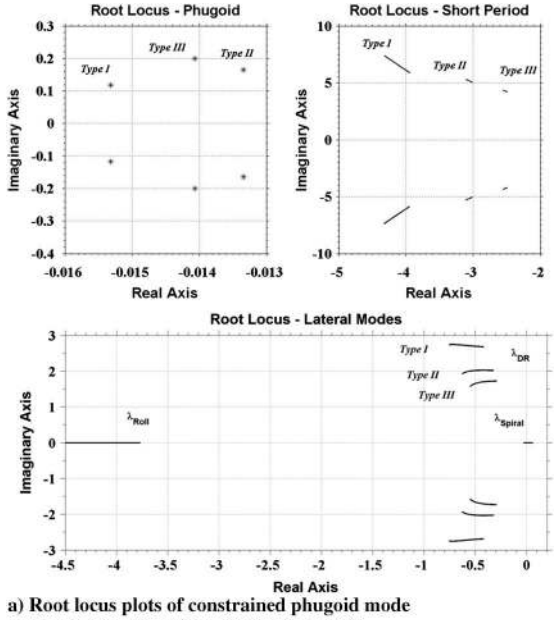

a) Root locus plots of constrained phugoid mode and unconstrained other modes of aircraft

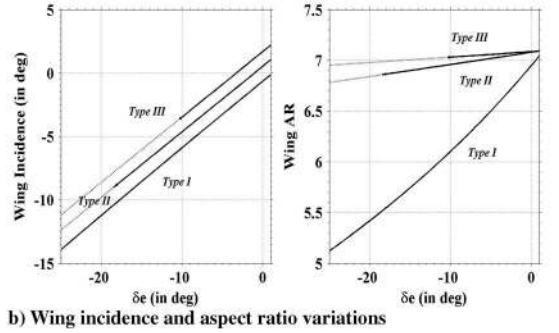

b) Wing incidence and aspect ratio variations

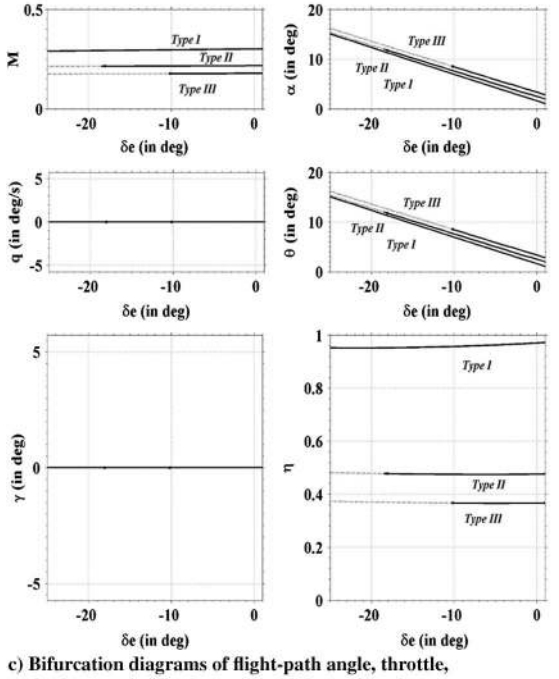

c) Bifurcation diagrams of flight-path angle, throttle, and other longitudinal-state variables as functions of the elevator deflection

Fig. 5 Root locus plots and bifurcation diagrams for phugoid mode control in straight and level flight trim condition.

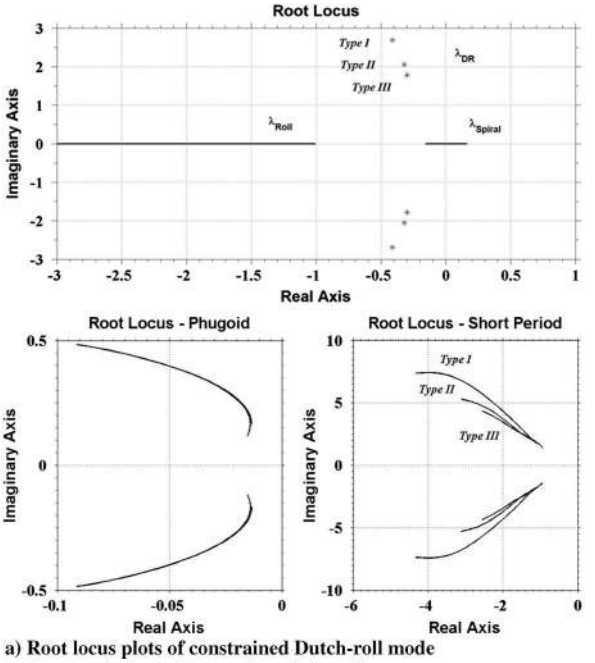

a) Root locus plots of constrained Dutch-roll mode and unconstrained other modes of aircraft

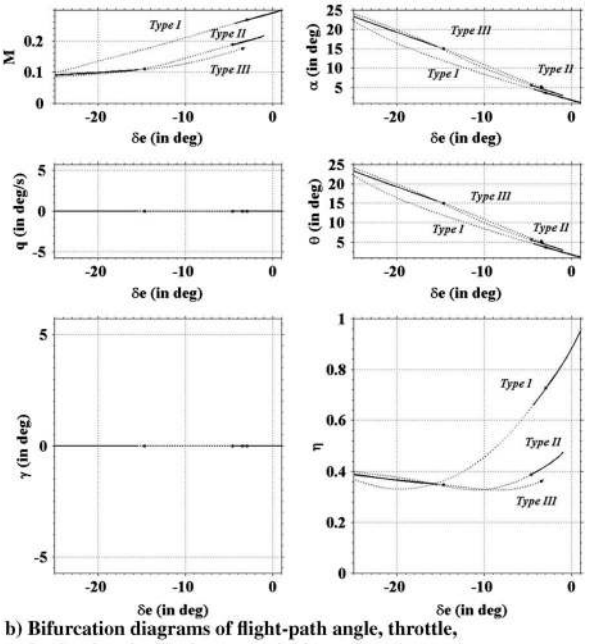

b) Bifurcation diagrams of flight-path angle, throttle, and other longitudinal-state variables as functions of the elevator deflection

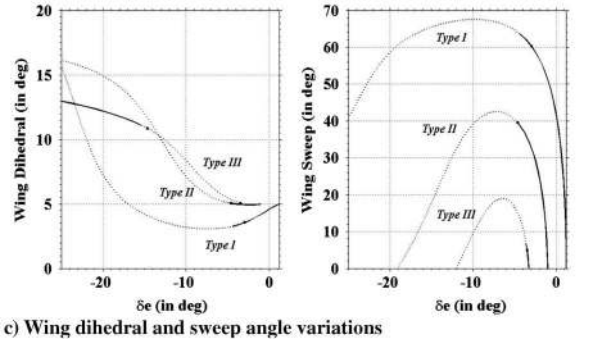

c) Wing dihedral and sweep angle variations

Fig. 6 Root locus plots and bifurcation diagrams for Dutch-roll mode control in straight and level flight trim condition.

The flight-path angle γ plot in Fig. 6b shows the imposed level-flight constraint. The schedules of wing dihedral and wing sweep angles are plotted in Fig. 6c. The trim solutions shown in Fig. 6b for types I and II have similar stability characteristics with all the solutions being stable at low angles of attack/elevator deflection and unstable at higher angles of attack/elevator deflections. The type III solution branch consists of

an unstable stretch (dotted line) due to the unstable spiral mode at lower angles of attack and a stable stretch (solid line) at higher angles of attack/elevator deflection. Trim solutions for the types I and II cases correspond to large sweep angles for Dutch-roll mode control and thus are not of practical interest. Thus, type III solutions are recommended for a lower throttle requirement and also for acceptable magnitudes of sweep and dihedral angles.

One of the important deductions from these computations is that the wing-morphing exercise does not ensure stability over the entire range of level-flight trim solutions, as is evident from the unstable spiral mode eigenvalues in both the cases. The use of vertical stabilizer parameters can be incorporated further for controlling the spiral mode in addition to controlling the Dutch-roll mode, which in turn would also have effects on the roll mode characteristics. All these complex studies can be carried out using the direct continuation methodology on a nonlinear aircraft model systematically without compromising on the rigor of analysis that such studies demand.

V. Conclusions

Development of the direct continuation methodology serves as a big step forward for the community of researchers dealing with problems of dynamical systems operating under constraints. A minor procedural change implemented in MATCONT, a MATLAB-based continuation algorithm, overcomes several drawbacks of the two-step EBA continuation procedure proposed earlier in the literature for the analysis of dynamical systems with constraints. The direct methodology is illustrated with application to three problems otherwise considered computationally challenging in aircraft flight dynamics. The direct methodology implemented in MATLAB is expected to allow users to make use of a host of other subroutines available in MATLAB to solve more challenging problems associated with multiparameter dynamical systems such as aircraft. Aircraft conceptual design, optimization, and control offer some such problems that one can expect to attempt within the framework of the direct methodology as shown in this paper through some examples.

As of now, not much significance of off-nominal solution branches originating from constrained solutions has been found, except that they indicate divergence from constrained conditions, which can be already deciphered from the type of bifurcations. If at all necessary, an additional step is required to compute off-nominal solution branches, as seen from the first example; this step still needs to be integrated with the direct methodology, which is part of an ongoing effort.

Appendix: Aircraft Rigid-Body Dynamics Equation

$$\dot{V} = \frac{1}{m}\left(T\cos\alpha\cos\beta - \frac{1}{2}\rho V^2 S C_D - mg\sin\gamma\right)$$

$$\dot{\alpha} = q - \frac{1}{\cos\beta}\left[(p\cos\alpha + r\sin\alpha)\sin\beta + \frac{1}{mV}\left(T\sin\alpha + \frac{1}{2}\rho V^2 S C_L - mg\cos\mu\cos\gamma\right)\right]$$

$$\dot{\beta} = \frac{1}{mV}\left(-T\cos\alpha\sin\beta + \frac{1}{2}\rho V^2 S C_Y + mg\sin\mu\cos\gamma\right) + (p\sin\alpha - r\cos\alpha)$$

$$\dot{p} = \left(\frac{I_{yy} - I_{zz}}{I_{xx}}\right)qr + \frac{1}{2I_{xx}}\rho V^2 S b C_l$$

$$\dot{q} = \left(\frac{I_{zz} - I_{xx}}{I_{yy}}\right)pr + \frac{1}{2I_{yy}}\rho V^2 S c C_m$$

$$\dot{r} = \left(\frac{I_{xx} - I_{yy}}{I_{zz}}\right)pq + \frac{1}{2I_{zz}}\rho V^2 S b C_n$$

$$\dot{\varphi} = p + q\tan\theta\sin\varphi + r\tan\theta\cos\varphi$$

$$\dot{\theta} = q\cos\varphi - r\sin\varphi$$

$$\sin\gamma = \cos\alpha\cos\beta\sin\theta - \sin\beta\sin\varphi\cos\theta - \sin\alpha\cos\beta\cos\varphi\cos\theta$$

$$\sin\mu\cos\gamma = \sin\theta\cos\alpha\sin\beta + \sin\varphi\cos\theta\cos\beta - \sin\alpha\sin\beta\cos\varphi\cos\theta$$

$$\cos\mu\cos\gamma = \sin\theta\sin\alpha + \cos\alpha\cos\varphi\cos\theta$$

References

[1] Strogatz, S. H., *Nonlinear Dynamics and Chaos*, Westview, Cambridge, MA, 1994, pp. 150–151.

[2] Cummings, P. A., "Continuation Methods for Qualitative Analysis of Aircraft Dynamics," NASA CR-2004-213035, 2014.

[3] Ananthkrishnan, N., and Sinha, N. K., "Level Flight and Trim Analysis Using Extended Bifurcation and Continuation Procedure," *Journal of Guidance, Control, and Dynamics*, Vol. 24, No. 6, 2001, pp. 1225–1228.
doi:10.2514/2.4839

[4] Sinha, N. K., and Ananthkrishnan, N., *Elementary Flight Dynamics with an Introduction to Bifurcation and Continuation Methods*, CRC Press, Boca Raton, FL, Oct. 2013, pp. 319–320.

[5] Doedel, E. J., Champneys, A. R., Fairgrieve, T., Kuznetsov, Y. A., Oldeman, B. E., Paffenroth, R., Sandstede, B., Wang, X., and Zhang, C., "AUTO-07P: Continuation and Bifurcation Software for Ordinary Differential Equations," Technical Rept., Concordia Univ., Montreal, Canada, 2008.

[6] Dhooge, A., Govaerts, W., and Kuznetsov, Y. A., "MATCONT: A MATLAB Package for Numerical Bifurcation Analysis of ODEs," *ACM Transactions on Mathematical Software*, Vol. 29, No. 2, 2003, pp. 141–164.
doi:10.1145/779359

[7] Kuznetsov, Y. A., *Elements of Applied Bifurcation Theory*, 2nd ed., Springer–Verlag, New York, 1998, p. 68.

[8] Sinha, N. K., and Ananthkrishnan, N., *Advanced Flight Dynamics with Elements of Flight Control*, CRC Press, Boca Raton, FL (to be published).

[9] Spetzler, M., and Narang-Siddarth, A., "Continuation Analysis of Nonlinear Systems with Equality Constraints on States, Parameters, and Eigenvalues," *Proceedings of the AIAA Guidance, Navigation and Control Conference, AIAA SciTech*, AIAA Paper 2015-1320, Jan. 2015.

[10] Narang, A., and Sinha, N. K., "Bifurcation Analysis as a Tool in Advanced Flight Testing," *Proceedings of the International Flight Test Seminar*, Aircraft Systems Testing Establishment, Bangalore, India, Feb. 2008, pp. 58–67.

[11] Stevens, B. L., and Lewis, F. L., *Aircraft Control and Simulation*, Wiley, Hoboken, NJ, 2003, pp. 291–308.

[12] Cook, M. V., *Flight Dynamics Principles*, 2nd ed., Elsevier Aerospace Engineering Series, Great Britain, U.K., 2007, pp. 165–167.

[13] Wang, Q., and Stengel, R. F., "Robust Nonlinear Flight Control of a High-Performance Aircraft," *IEEE Transactions on Control Systems Technology*, Vol. 13, No. 1, 2005, pp. 15–26.
doi:10.1109/TCST.2004.833651

[14] Abdulhamitbilal, E., and Jafarov, E. M., "Robust Sliding Mode Speed Hold Control System Design for Full Nonlinear Aircraft Model with Parameter Uncertainties: A Step Beyond," *Proceedings of the 12th IEEE International Workshop on Variable Structure Systems (VSS 2012)*, IEEE Publ., Piscataway, NJ, Jan. 2012, pp. 7–15.

[15] Andry, A. N., Shapiro, E. Y., and Chung, J. C., "Eigenvalue/Eigenvector Assignment Using Output Feedback," *IEEE Aerospace and Electronic Systems Magazine*, Vol. AES-19, No. 5, 1983, pp. 711–729.
doi:10.1109/TAES.1983.309373

[16] Nelson, R. C., *Flight Stability and Automatic Control*, McGraw–Hill, New York, 1997, pp. 347–355.

[17] Neil, D. A., III, "Design, Development and Analysis of a Morphing Aircraft Model for Wind Tunnel Experimentation," Master's Thesis, Virginia Polytechnic Inst. and State Univ., Blacksburg, VA, 2006.

[18] Khatri, A. K., Singh, J., and Sinha, N. K., "Aircraft Design Using Constrained Bifurcation and Continuation Method," *Journal of Aircraft*, Vol. 51, No. 5, 2014, pp. 1647–1653.
doi:10.2514/1.C032288

[19] Raymer, D. P., *Aircraft Design: A Conceptual Approach*, AIAA Education Series, AIAA, Washington, D.C., 1992.

[20] Pamadi, B. N., *Performance, Stability, Dynamics, and Control of Airplanes*, AIAA Education Series, AIAA, Reston, VA, 2004.